Synergistic freshwater and electricity production using passive membrane distillation and waste heat recovered from camouflaged photovoltaic modules

Supplementary material for

Synergistic freshwater and electricity production using passive membrane distillation and waste heat recovered from camouflaged photovoltaic modules

Giovanni Antonetto[a], Matteo Morciano[a,b], Matteo Alberghini[a,b], Gabriele Malgaroli[a], Alessandro Ciocia[a], Luca Bergamasco[a], Filippo Spertino[a], Matteo Fasano[a,b,*]

[a] *Department of Energy, Politecnico di Torino, Corso Duca degli Abruzzi 24, 10129 Torino, Italy*
[b] *Clean Water Center, Politecnico di Torino, Corso Duca degli Abruzzi 24, 10129 Torino, Italy*

[*] Corresponding author
Email address: matteo.fasano@polito.it (Matteo Fasano)

Supplementary note 1

This note reports some pictures showing in detail the design and production development of the prototype.

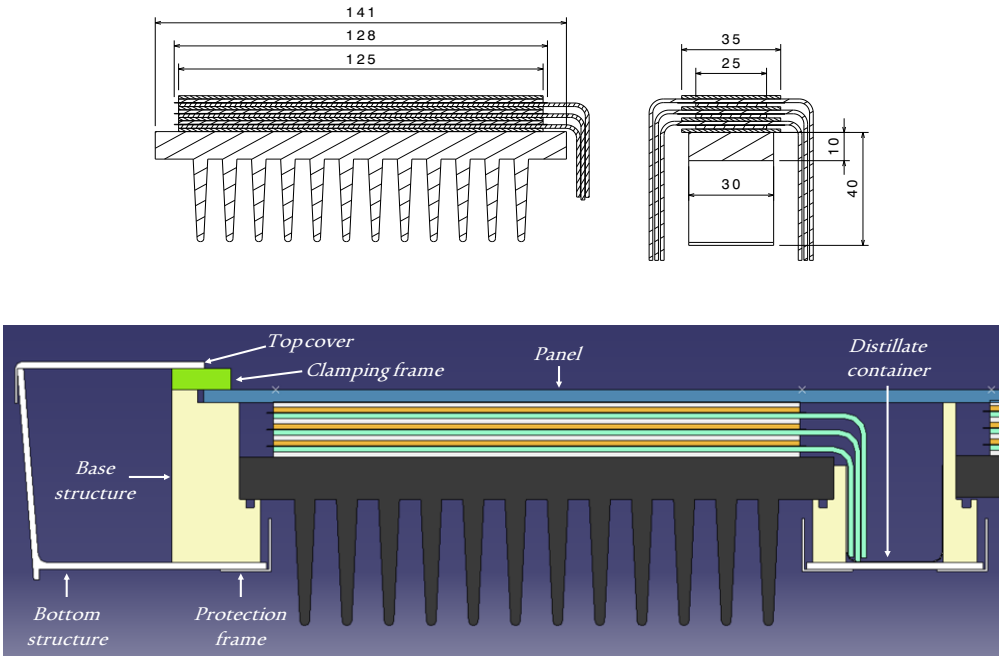

Figure S1: Sections of a single distiller module (top), dimensions are indicated in [mm]; detailed section of the prototype assembly (bottom).

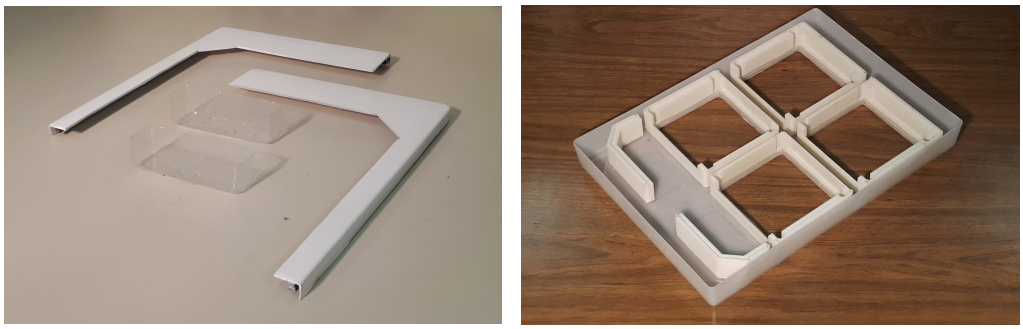

Figure S2: Thermoformed components of the prototype: white top cover and distillate containers (left); assembled parts of the structure supporting the eight distillers below the four PV cells (right).

Supplementary note 2

The performance of PV modules is typically referred to Standard Test Conditions (STC), with solar irradiance G_{STC} = 1000 W m^{-2}, mean temperature of the cells T_{STC} = 25 °C and solar spectrum AM1.5. However, since the measurements are usually not carried out under the prescribed external conditions, International Standards [1] define a procedure to correct the acquired current and voltage to STC. In particular, the short-circuit current I_{sc} is assumed proportional to G, while the open-circuit voltage V_{oc} depends on temperature T_{cell} by means of a coefficient β, usually provided by the manufacturer at constant irradiance [2, 3]:

$$V_{\mathrm{oc}}(T_{\mathrm{cell}}) = V_{\mathrm{oc,STC}} \cdot \left[1 + \beta \cdot (T_{\mathrm{cell}} - T_{\mathrm{STC}})\right], \tag{S1}$$

where $V_{\mathrm{oc,STC}}$ is the open-circuit voltage in STC and generally $\beta \approx -0.3$ % K^{-1} [4]. Moreover, for operating conditions different from STC, the maximum output power P_{mpp} of PV generators is estimated with the following equation:

$$P_{mpp}(G, T_{cell}) = \frac{G}{G_{STC}} \cdot P_{mpp,STC} \cdot \left[1 + \gamma \cdot (T_{cell} - T_{STC})\right], \tag{S2}$$

where $P_{\mathrm{mpp,STC}}$ is the rated power at STC and γ is the temperature coefficient for power, generally ranging between −0.45 % K^{-1} and −0.35 % K^{-1} for commercial PV modules [2, 5]. Regarding the efficiency η_{PV} of a PV generator, it is generally constant for $G > 600$ W m^{-2} [6] and calculated starting from the rated efficiency at STC (η_{STC}) using the following expression:

$$\eta_{PV}(T_{cell}) = \eta_{STC} \cdot \left[1 + \gamma \cdot (T_{cell} - T_{STC})\right]. \tag{S3}$$

The temperature coefficients β and γ of the tested PV module have been estimated from the experiments described in Section 3.3, and compared with typical values used for commercial PV generators. In the last part of the analysis, the currents have been corrected to STC, while no correction has been applied to the voltages. Starting from these curves, the electrical efficiency has been estimated for the measurement conditions, in order to evaluate the effect of temperature on PV performance.

Supplementary note 3

The Mackie-Meares equation models the correlation between porosity and tortuosity as:

$$\tau = \frac{(2-\epsilon_{\mathrm{m}})^2}{\epsilon_{\mathrm{m}}}. \tag{S4}$$

The vapour pressure differential is calculated via Raoult's law as:

$$\Delta p_{\mathrm{v}} = a(Y_{\mathrm{eva}})p_{\mathrm{v}}(T_{\mathrm{eva}}) - a(Y_{\mathrm{cond}})p_{\mathrm{v}}(T_{\mathrm{cond}}). \tag{S5}$$

Raoult's law shows the effect of salinity and temperature on the overall vapour pressure gradient. To evaluate the activity, the following expression is adopted:

$$a(Y) = \frac{m_{\mathrm{NaCl}}(1-Y)}{m_{\mathrm{NaCl}}(1-Y) + n_{\mathrm{ion}} m_{\mathrm{w}} Y}, \tag{S6}$$

where m_{NaCl} is the molar mass of sodium chloride and $n_{\mathrm{ion}} = 2$. For a feed water salinity of 35 g/l, $Y_{\mathrm{eva}} = 0.035$ and hence $a(Y_{\mathrm{eva}}) = 0.978$, while for distilled water $a(Y_{\mathrm{C}}) = 1$. This implies that a more saline solution reduces the performance of the distiller. The vapour pressures of pure water can be calculated using Antoine's correlation [7]:

$$p_{\mathrm{v}}(T) = \exp\left(23.1964 - \frac{3816.44}{T - 46.13}\right), \tag{S7}$$

with p_{v} in Pa and T in K. The model considers the effective transmittance of the membrane U_{mem} as follows:

$$U_{\mathrm{mem}} = \left(\frac{d_{\mathrm{m}}}{\epsilon_{\mathrm{m}} \cdot k_{\mathrm{a}} + (1-\epsilon_{\mathrm{m}}) \cdot k_{\mathrm{PTFE}}} + \frac{d_{\mathrm{a}}}{k_{\mathrm{a}}}\right)^{-1}, \tag{S8}$$

with the thermal conductivity of PTFE equal to $k_{\mathrm{PTFE}} = 0.25$ W m^{-1} K^{-1} and that of air to $k_{\mathrm{a}} = 0.026$ W m^{-1} K^{-1}.

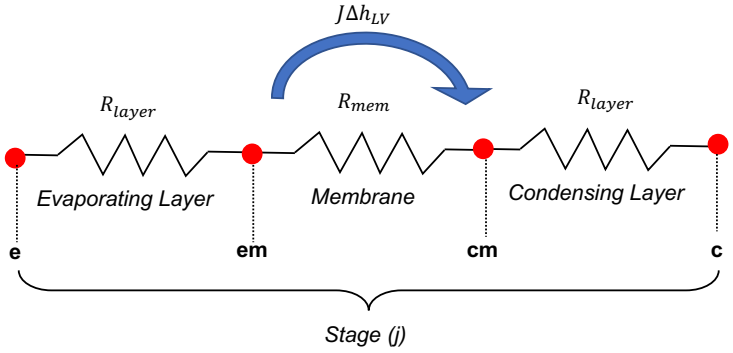

Figure S3: Equivalent thermal circuit of one stage of the distiller. Note that part of the heat is transferred via mass transport through the product $J\Delta h_{\mathrm{LV}}$.

Supplementary note 4

3D Finite Elements Method model

The reference conditions and parameters considered for the FEM model are the following: G = 1000 W m^{-2}, temperature of the saltwater T_w = 20 °C, ambient temperature T_{amb} = 35 °C, average convective heat transfer coefficient h_a = 5 W m^{-2} K^{-1} and heat transfer coefficient of the heat sink U_{out} = 334 W m^{-2} K^{-1}. The infrared picture in Fig. S4a shows the cooling effect of the distiller on the bottom side of the PV panel. The 3D FEM simulation estimates that the cooled area of the panel has a temperature of ≈ 57 °C, whereas far away it reaches 75 °C as shown in Fig. S4b. Fig. S4c shows a temperature field similar to the experimental one reported in Fig. 7c, with the first aluminium plate at ≈ 49 °C and the last at 22.5 °C. Fig. S4d shows how the vertical heat flux is more intense in the narrow sections, measuring around 1100 W m^{-2}, while it is negligible on the sides of the wide sections. It is worth to point out that the pictures representing the results of the numerical simulations (namely, Figs. S4c, S4d) are referred to a longitudinal section of the 3D simulation domain. At the contact between the panel and the first aluminium plate it is possible to note the concentration of the flux from a wider to a narrower section. The model allows to evaluate the net incoming heat flux in the distiller, that is q_{in} = 786 W m^{-2}.

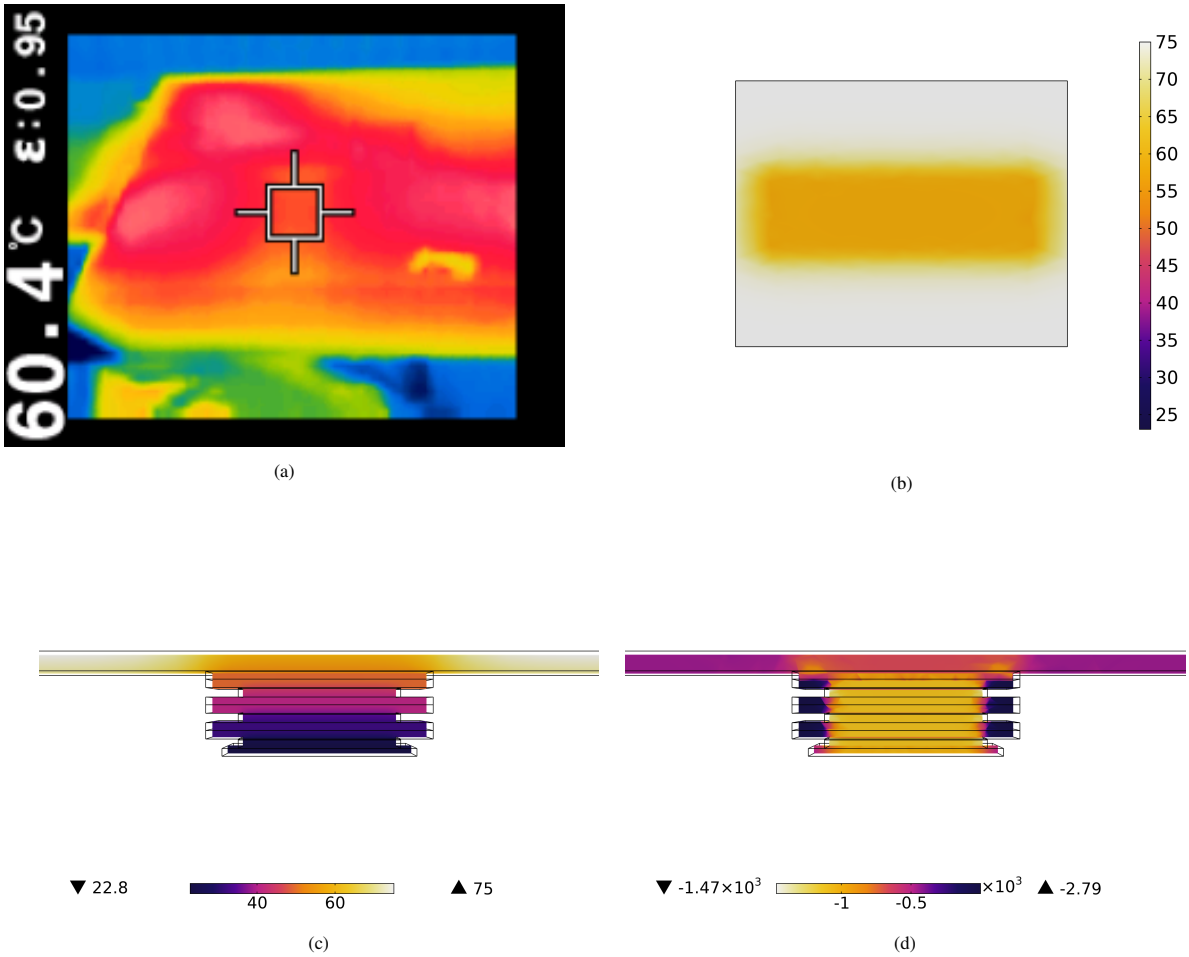

Figure S4: Thermal study of the coupled prototype. (a) Infrared picture of the PV module during experiments under 1 sun: the orange shape represents the surface of the PV module cooled beneath by the distiller. (b) Simulated temperature field (expressed in °C) on the top surface of the PV module. The simulation allows to compute the (c) temperature (expressed in °C) and (d) vertical heat flux (expressed in W m^{-2}) fields in a longitudinal section of the domain. The heat flux sign is negative because it is directed downwards.

Emissivity of the PV module

The emissivity of the solar panel is measured in the infrared region using a thermal camera. A thermocouple is used to measure the temperature of the heated sample. Then, this value is compared with the temperature measured by the camera's sensor in order to infer the emissivity. As shown in Fig. S5, the temperature of the panel reached an average steady state value of $T_{\text{panel}} = 63.1$ °C during the test, which corresponds to an emissivity $\varepsilon = 0.95$.

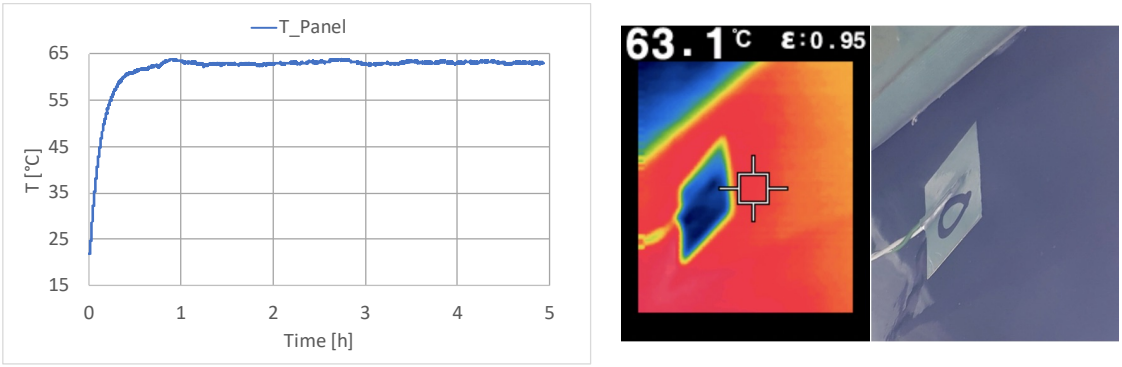

Figure S5: Emissivity characterization: temperature profile during the test (left); infrared and visible light pictures of a thermocouple placed on the panel (right).

Transmittance of the distiller

The overall thermal transmittance of the distiller is calculated as follows:

$$U_{\text{dist}} = \frac{q_{\text{in}}}{\bar{T}_{\text{eva,1}} - T_{\text{wb}}} = 25.42 \text{ W m}^{-2} \text{ K}^{-1}, \tag{S9}$$

being $q_{\text{in}} = 786$ W m^{-2}, $\bar{T}_{\text{ev,1}} = 51.0$ °C (average temperature of the surface of the first evaporator in contact with the PV module) and $T_{\text{wb}} = 20.0$ °C (temperature of the saltwater in the feeding basin). Then, U_{dist} is used in the simplified FEM model as shown in Fig. S6.

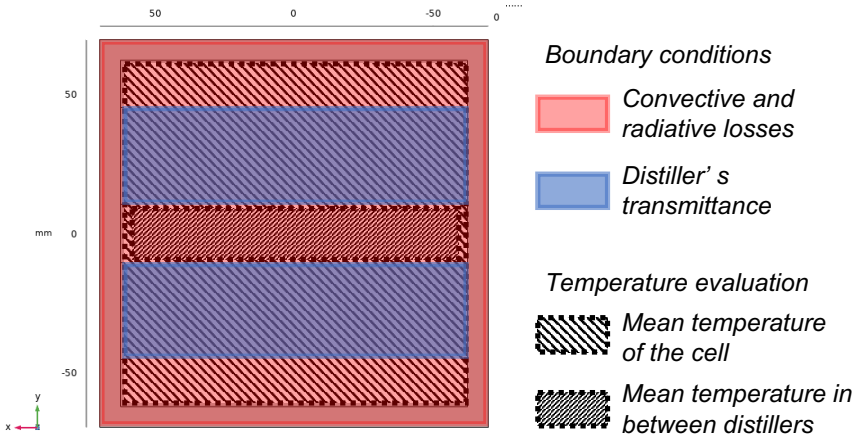

Figure S6: Bottom surface of the simplified FEM model. Convective and radiative losses are applied on the red area, while the thermal transmittance of the distillers on the blue area. The mean temperature of the PV cell is obtained by calculating the average temperature over the 125 mm × 125 mm surface with large dashed lines. The mean temperature between the distillers is obtained calculating the average temperature over the surface with narrow dashed lines.

Model parameters

Minimum and maximum values for the variables used in the numerical model have been adopted to determine the uncertainty of the estimations (see the Tab. S1 below). Upper and lower bounds have been inferred from experimental evidence. The value of solar flux I_{rr} is affected by uncertainty due to non uniformity of the beam, accounting for $\pm$ 51.3 W m^{-2}, namely the standard deviation of the irradiance measured in several points during the calibration of the solar simulator. This value is in agreement with that reported in the data-sheet of the solar simulator (maximum deviation of $< \pm$ 5%). h_{a} is estimated via calculation of natural and forced convection at low air speeds. The thickness of the additional air gap (d_a) between membrane and cloths, which considers their non-ideal contact, ranges from 65 μm to 85 μm. ϵ_m is taken from Refs. [8, 9].

Table S1: Ranges of input variables used in the simulations.

	I_{rr} [W m^{-2}]	h_{a} [W m^{-2} K^{-1}]	d_{a} [μm]	ϵ_{m} [$-$]
min	950	3	65	0.75
max	1050	7	85	0.85

Supplementary note 5

Table S2: Overview of the key figures of merit of commercial renewable desalination technologies. The meaning of the acronyms are: Solar Distillation (SD); Multiple Effect Distillation (MED); Concentrated Solar Power (CSP); Membrane Distillation (MD); PV (Photovoltaic); Reverse Osmosis (RO); Electrodialysis (ED); Seawater (SW); Brackish water (BW). Data taken from from Ref. [10].

RENEWABLE WATER DESALINATION							
Technology	**SD**	**Solar MED**	**Solar MD**	**Solar CSP/MED**	**PV/RO**	**PV/ED**	**Wind/RO**
Development Status	Appl.	Appl./R&D	R&D	R&D	Appl./R&D	R&D	Appl./R&D
Energy input kWh_e/m^3	Solar	1.5	0	1.5-2	0.5-1.5 BW	3-4 BW	0.5-1.5 BW
$+kWh_t/m^3$	passive	+ 27.8	+ 55.6	+ 16.7-19.4	4-5 SW + 0	+ 0	4-5 SW + 0
Current capacity m^3/day	0.1	1-100	0.1-100	>5000	<100	<100	50-20000
Production cost $/$m^3$	1.3-6.5	2.6-6.5	10.4-19.5	2.3-2.9	6.5-15.6	10.4-11.7	3.9-9.1

Supplementary note 6

A Strengths-Weaknesses-Opportunities-Threats (SWOT) analysis of the proposed coupling between a camouflaged PV panel and a passive multi-stage distillation device is reported below.

	Helpful	Harmful
Internal factors	**Strengths** • Freshwater – electricity cogeneration • Modular assembly: high flexibility • Distiller: low-cost design • Distiller: low and easy maintenance • PV panel: increased performance • PV panel: low visual impact	**Weaknesses** • Distiller: manual assembly of several components • Lab-scale prototype (TRL 3-4) • Visual texture slightly reduces the PV efficiency
External factors	**Opportunities** • Ideal for off-grid and/or floating installations • Ability to treat a wide range of wastewaters • Environmental conditions have low impact on the distiller performance • Frugal design: easy replacement of components	**Threats** • No-self cleaning: dust and dirt might lower the PV performance • Maintenance of PV panel requires skilled workforce

Figure S7: SWOT analysis of the presented synergistic freshwater and electricity production system.

References

[1] IEC 60891:2009, Photovoltaic devices - Procedures for temperature and irradiance corrections to measured I-V characteristics.

[2] S. B. Schujman, J. R. Mann, G. Dufresne, L. M. LaQue, C. Rice, J. Wax, D. J. Metacarpa, P. Haldar, Evaluation of protocols for temperature coefficient determination, in: 2015 IEEE 42nd Photovoltaic Specialist Conference (PVSC), IEEE, 2015, pp. 1–4.

[3] P. Di Leo, F. Spertino, S. Fichera, G. Malgaroli, A. Ratclif, Improvement of self-sufficiency for an innovative nearly zero energy building by photovoltaic generators, in: 2019 IEEE Milan PowerTech, IEEE, 2019, pp. 1–6.

[4] R. Dubey, P. Batra, S. Chattopadhyay, A. Kottantharayil, B. M. Arora, K. Narasimhan, J. Vasi, Measurement of temperature coefficient of photovoltaic modules in field and comparison with laboratory measurements, in: 2015 IEEE 42nd Photovoltaic Specialist Conference (PVSC), IEEE, 2015, pp. 1–5.

[5] S. Liu, M. Dong, Quantitative research on impact of ambient temperature and module temperature on short-term photovoltaic power forecasting, in: 2016 International Conference on Smart Grid and Clean Energy Technologies (ICSGCE), IEEE, 2016, pp. 262–266.

[6] M. Donovan, B. Bourne, J. Roche, Efficiency vs. irradiance characterization of pv modules requires angle-of-incidence and spectral corrections, in: 2010 35th IEEE Photovoltaic Specialists Conference, IEEE, 2010, pp. 002301–002305.

[7] M. Khayet, T. Matsuura, Membrane distillation: principles and applications (2011).

[8] E. Chiavazzo, M. Morciano, F. Viglino, M. Fasano, P. Asinari, Passive solar high-yield seawater desalination by modular and low-cost distillation, Nature sustainability 1 (12) (2018) 763–772.

[9] M. Morciano, M. Fasano, L. Bergamasco, A. Albiero, M. L. Curzio, P. Asinari, E. Chiavazzo, Sustainable freshwater production using passive membrane distillation and waste heat recovery from portable generator sets, Applied Energy 258 (2020) 114086.

[10] M. Isaka, Water desalination using renewable energy technology brief, IEA-ETSAP and IRENA© Technology Brief I12–March (2012).